15 Feb 2014

The Structure And Properties Of Zinc Aluminophosphate Glasses

Charmayne E. Smith (Lonergan)
Missouri University of Science and Technology, clonergan@mst.edu

Richard K. Brow
Missouri University of Science and Technology, brow@mst.edu

Lionel Montagne

Bertrand Revel

Recommended Citation

C. E. Smith (Lonergan) et al., "The Structure And Properties Of Zinc Aluminophosphate Glasses," *Journal of Non-Crystalline Solids*, vol. 386, pp. 105 - 114, Elsevier, Feb 2014.
The definitive version is available at https://doi.org/10.1016/j.jnoncrysol.2013.11.042

Journal of Non-Crystalline Solids 386 (2014) 105–114

Contents lists available at ScienceDirect

Journal of Non-Crystalline Solids

journal homepage: www.elsevier.com/ locate/ jnoncrysol

The structure and properties of zinc aluminophosphate glasses

Charmayne E. Smith [a], Richard K. Brow [a,*], Lionel Montagne [b], Bertrand Revel [b]

[a] Missouri University of Science and Technology, Rolla, MO 65409, USA
[b] Université de Lille 1, Sciences et Technologies, Unité de Catalyse et de Chimie du Solide —UMR CNRS 8181, 59655 Villeneuve d'Ascq, France

ARTICLE INFO

Article history:
Received 26 October 2013
Received in revised form 25 November 2013
Available online 21 December 2013

Keywords:
Aluminophosphate glasses;
Nuclear magnetic resonance;
Zinc phosphate glasses;
Structure;
Properties

ABSTRACT

The glass forming region of the ZnO–Al_2O_3–P_2O_5 (ZAP) system was determined and the structures and properties of the glasses were characterized. For glasses with a constant O/P ratio, i.e., with similar average phosphate anion distributions, and with increasing alumina content, there is an increase in molar volume and glass transition temperature and a decrease in density and refractive index. The structures of the ZAP glasses were characterized by Raman spectroscopy, ^{31}P and ^{27}Al magic angle spinning (MAS) nuclear magnetic resonance (NMR) spectroscopy, and high pressure liquid chromatography (HPLC). Systematically shorter phosphate anions constitute the structures of glasses with greater O/P ratios. The average aluminum coordination number (CN_{Al}) changes systematically with composition, from ~4.0 to ~5.6, depending on the number of terminal oxygens available to coordinate each Al-cation. Glass properties are sensitive to both the types and concentrations of the P-anions as well as the CN_{Al}.

1. Introduction

Zinc phosphate glasses have been developed for a variety of applications, including low temperature seals [1–3] and as hosts for luminescent ions [4–6]. More recently, it has been shown that the optical properties of zinc phosphate glasses can be modified with a femto-second laser [7–12], making these glasses candidates for a variety of optical devices.

There have been many studies of the structures and properties of binary Zn-phosphate glasses [13–27]; glasses with the nominal molar composition $xZnO \cdot (1-x)P_2O_5$ have been made with up to 80 mol% ZnO [26]. Kordes classified the $xZnO \cdot (1-x)P_2O_5$ system as anomalous because of discontinuities in the composition–property relationships near $x = 0.5$, the metaphosphate composition [13]. It has been argued that such breaks indicate changes in the Zn coordination environment; e.g., the Zn coordination number decreases from 6 to 4 with an increase of the ZnO content to 50 mol% [14,15]. However, diffraction studies completed more recently indicate a preference for tetrahedral Zn coordination for glasses with ZnO contents from 45 to 65 mol% [21] and for glasses with ZnO concentrations greater than 50 mol% [23,28].

Phosphate anionic structures can be described using the Q^n-terminology, where 'n' represents the number of bridging oxygens on a phosphate tetrahedron [19]. For example, changes in the types of phosphate tetrahedra with the addition of ZnO can be represented by the reaction:

$$2Q^n + ZnO \rightarrow 2Q^{n-1}. \quad (1)$$

Here, the oxygen ions accompanying the ZnO added to phosphate glasses replace bridging oxygens (P–O–P) with nonbridging oxygens (P–O–Zn) on the phosphate tetrahedra.

The structures of binary Zn-phosphate (ZP) glasses have been studied by infrared [17,18] and Raman [17,18,20,26] spectroscopies, ^{31}P NMR [20,25,26], X-ray photoelectron spectroscopy (XPS) [16,27], and high pressure liquid chromatography (HPLC) [24,26]. For glasses with increasing ZnO-content (increasing O/P ratio), the average phosphate anion becomes shorter as described by Eq. (1). For compositions with higher O/P ratios, especially near the pyrophosphate stoichiometry ($x = 0.67$, $O/P = 3.5$), the glasses possess a broader range of P-tetrahedra than are expected from Eq. (1). Disproportionation reactions like the one shown here occur in these melts to produce glasses with more complex structures:

$$2Q^1 \rightarrow Q^0 + Q^2. \quad (2)$$

The broader distribution of phosphate anions that results from such disproportionation reactions may contribute to the larger glass forming range typical of the binary zinc phosphate system.

A disadvantage of the binary zinc phosphate glasses is their relatively poor chemical durability. The bonds between Zn polyhedra and P-anions are readily hydrolyzed, leading to the rapid degradation of the glass surface [29]. Koudelka and others have shown that with the addition of certain oxides, for example B_2O_3 and Nb_2O_5 [30–32], more hydrolytically stable linkages form between the phosphate anions, improving chemical durability.

It has long been known that the addition of alumina to a phosphate glass improves its chemical durability [33]. Brow et al. showed that the coordination environments of Al-cations, and so the properties,

* Corresponding author. Tel.: +1 573 341 6812.
E-mail address: brow@mst.edu (R.K. Brow).

0022-3093/$ – see front matter © 2013 Elsevier B.V. All rights reserved.
http://dx.doi.org/10.1016/j.jnoncrysol.2013.11.042

of sodium aluminophosphate glasses depend on the O/P ratio [34,35]. More recent structural studies of Ca- [36] and other ternary aluminophosphate glasses [37] show similar compositional dependences of the Al coordination environments.

Fu et al. recently reported the density, molar volume, refractive index and Raman spectra for three glasses in the zinc aluminophosphate (ZAP) system, doped with small amounts of terbium oxide [38], while others have studied the luminescence properties of ZAP glasses co-doped with Tm_2O_3 and Dy_2O_3 [5]. Interestingly, there does not appear to be any systematic study of the properties and structures of glasses from the ternary $ZnO–Al_2O_3–P_2O_5$ system. The purpose of this paper then is to report the glass-forming range for ZAP compositions with O/P > 3, to describe useful properties, and to provide information about their compositionally-dependent structures.

2. Experimental procedures

Zinc aluminophosphate (ZAP) glasses were prepared by batching appropriate mixtures of $NH_4H_2PO_4$ (ACS, 98.0%—Alfa Aesar), ZnO (reagent grade, ≥99.0%—Sigma-Aldrich), Al_2O_3 (99.5% metals basis—Alfa Aesar) and/or aluminum metaphosphate (Alfa Aesar) to produce 15–25 g of glass. The batches were thoroughly mixed, calcined in high purity alumina crucibles (AdValue Technology, 99.9%) for 15–18 h at 500 °C to evolve water and NH_3, then melted at temperatures between 1000 and 1500 °C for 1–3 h, depending on the composition. For glasses melted above 1275 °C, the crucibles were covered with alumina discs to minimize P_2O_5 loss. Melts were quenched by pouring into cylindrical steel molds (10 mm in diameter and 25 mm tall) when possible, or by quenching between two copper plates. Samples were annealed near their glass transition temperatures (T_g) for 2 h. The glass-forming region described in this work is defined as those compositions which form X-ray amorphous glasses from melts with a maximum melting temperature of 1500 °C.

Annealed samples, 10 mm in diameter and ~1 mm thick, were polished to a 1200 grit (~5 μm) finish for optical measurements. Refractive index at 632.8 nm was measured using a prism coupler (Metricon model 2010/M); the uncertainty of these measurements is ±0.0004.

The density of annealed glass samples was measured by Archimedes' method using distilled water as the immersion liquid. Three samples of each glass were measured and the standard deviation was recorded (typically ±0.008 g/cm^3). The molar volume was calculated by dividing the density of each glass by the molecular mass, calculated from the analyzed glass compositions, of polished samples, as determined by a Helios NanoLab 600 FIB/FESEM equipped with an energy dispersive spectrometer. The intensities of the Zn–Kα, Al–Kα, P–Kα lines were determined from at least three different areas on each sample, converted to the relative concentration of each respective oxide using the system sensitivity factors, and the average compositions are reported. Three different pieces of several samples were analyzed in a similar manner, and from these analyses, the overall estimated relative uncertainty of the reported compositions is ±2.5%.

Glass transition temperatures (T_g) were determined by differential thermal analysis (DTA, Perkin-Elmer DTA-7) by heating 35–40 mg of glass powders (<75 μm) at 10 °C/min in high purity, open alumina crucibles under a nitrogen flow. The onset method was used to determine T_g and the estimated uncertainty is ±5 °C.

The coefficient of thermal expansion (CTE) was measured on glass cylinders using an Orton dilatometer, model 1600D, with a heating rate of 10 °C/min. The CTE values were determined as the slope of the linear fit of the dilatometry data between 200 and 400 °C and were reproducible to ±0.2 ppm/°C.

Weight loss measurements were made on bulk glasses to determine relative chemical durability in deionized (DI) water at room temperature (~20 °C) for up to 170 h. Polished samples (~5 μm) were rinsed with acetone and dried before testing. A constant sample surface area (SA) to solution volume ratio of 0.035 cm^{-1} was used for each experiment. Samples were removed from the water periodically, dried and weighed, and then returned to the solution. Three samples were tested for each condition and the average weight loss is reported.

Raman spectra were collected with a Horiba-Jobin Yvon LabRam spectrometer between 100 and 1500 cm^{-1} using a HeNe laser (632.8 nm) as the excitation source.

Magic Angle Spinning (MAS) Nuclear Magnetic Resonance (NMR) spectroscopy was performed with a Bruker spectrometer with magnetic field strengths of 9.4 T and 18.8 T for ^{31}P and ^{27}Al spectra, respectively. The ^{31}P spectra were collected in 8 scans with a spinning rate of 12,500 Hz, a relaxation delay equal to 120 s and a pulse length of 2.38 μs. The ^{27}Al spectra were collected in 512 scans, 2 s relaxation delay, pulse length of 1 μs and a spinning rate of 20,000 Hz. ^{31}P and ^{27}Al chemical shifts were referenced to 85% H_3PO_4 and 0.1 M $AlCl_3$ solutions, respectively. The decomposition of the NMR spectra was carried out using the DM-FIT software [39]. The distribution of quadrupolar parameters of the ^{27}Al nucleus induces an asymmetric line shape of the resonances, which has been fitted with the Czjzek distribution model of the DMFit software [40].

High pressure liquid chromatography was done to characterize phosphate anion distributions using a Dionex GP50-2 pump, an AD25 absorbance detector and an Ionpack AS7 4 × 250 mm Analytical Ion exchange column. Samples were ground to <53 μm particle size and dissolved in a solution of 5 mM EDTA and 0.22 M NaCl (pH = 10) for 1–3 h and analyzed within 24 h. Chromatographs were collected with a linear solution gradient from 0.053 M NaCl to 0.5 M NaCl, both with 5 mM EDTA. Further information about these types of HPLC measurements can be obtained elsewhere [24,41].

3. Results

Table 1 lists the processing temperatures and times, as well as the as-batched and analyzed (EDS) compositions of the ZAP glasses prepared for this study. Due to the loss of P_2O_5 and the transfer of Al_2O_3 from the alumina crucibles, especially at the higher processing temperatures, the analyzed compositions deviate from the batched compositions.

Table 1
Compositions, melting time and melting temperature of the $ZnO–Al_2O_3–P_2O_5$ glasses.

Sample ID	Batched values [mol%]			Analyzed values [mol%]				Melting conditions
Glass designation[a]	ZnO	Al_2O_3	P_2O_5	ZnO	Al_2O_3	P_2O_5	O/P ratio	Temp [°C]/ time [h]
46-2-52_2.99	30.0	0.0	70.0	46.4	1.5	52.1	2.99	1000/1
49-2-49_3.05	50.0	0.0	50.0	48.5	2.1	49.4	3.05	1200/3
47-3-50_3.08	20.0	0.0	80.0	46.9	3.4	49.7	3.07	1200/2
38-7-55_3.04	40.0	5.0	55.0	38.2	7.1	54.7	3.04	1280/3
33-11-56_3.10	30.0	10.0	60.0	33.2	11.1	55.7	3.10	1250/3
27-16-57_3.15	20.0	13.0	67.0	26.9	15.7	57.4	3.15	1350/3
22-18-60_3.14	10.0	10.0	80.0	21.7	18.4	59.9	3.14	1400/3
0-29-71_3.12	0.0	25.0	75.0	0.0	29.4	70.6	3.12	1500/1
55-3-43_3.23	55.0	0.0	45.0	54.6	2.6	42.8	3.23	1100/3
52-4-43_3.26	50.0	3.0	47.0	52.4	4.4	43.2	3.26	1100/3
40-11-49_3.24	39.0	10.0	51.0	40.5	10.6	48.8	3.24	1250/3
25-19-57_3.26	25.0	15.0	60.0	24.8	18.7	56.5	3.22	1350/3
26-19-55_3.26	20.0	15.0	65.0	26.1	19.1	54.8	3.26	1400/3
13-25-62_3.22	10.0	20.0	70.0	13.4	25.0	61.6	3.22	1450/3
0-34-66_3.27	0.0	27.0	73.0	0.0	34.0	66.0	3.27	1500/1
51-6-43_3.30	51.0	5.0	44.0	50.9	6.1	43.0	3.30	1250/3
44-11-45_3.34	42.0	10.0	48.0	44.1	10.7	45.2	3.34	1250/3
36-15-49_3.32	33.0	15.0	52.0	36.1	14.9	49.0	3.32	1350/3
28-20-52_3.35	24.0	20.0	56.0	28.3	19.9	51.8	3.35	1450/3
61-3-37_3.44	60.0	0.0	40.0	60.5	2.8	36.7	3.44	1150/3
58-5-37_3.50	58.3	5.0	36.7	58.2	5.1	36.7	3.50	1175/3
55-6-39_3.45	55.0	5.0	40.0	55.0	6.3	38.7	3.45	1300/3
64-3-34_3.56	66.7	0.0	33.3	63.5	2.7	33.8	3.56	1100/1
64-3-33_3.63	65.0	0.0	35.0	64.1	3.3	32.6	3.63	1250/2
70-2-29_3.81	70.0	0.0	30.0	70.0	1.6	28.5	3.81	1075/2

[a] In mol%, $ZnO–Al_2O_3–P_2O_5$_O/P ratio.

Fig. 1 shows the glass forming range based on the analyzed compositions. Batches that were un-melted at 1500 °C, or that crystallized on cooling, are shown as squares (red) in Fig. 1. (These symbols represent nominal compositions, not analyzed.). No alumina-free glasses were prepared because of alumina-transfer from the crucible, and no ultraphosphate compositions were synthesized with O/P ratios less than 3.0 (blue line in Fig. 1) because of alumina transfer and the loss of P_2O_5 from the melts. The maximum concentrations of ZnO and Al_2O_3 were about 70 mol% and 34 mol%, respectively. These values are similar to the glass forming limits that were previously established in studies of the binary zinc phosphate [26] and aluminophosphate [42–44] systems. The reported glass forming ranges for these binary systems are also indicated in Fig. 1.

3.1. Glass properties

Weight loss data for a series of ZAP glasses with similar O/P ratios of 3.32 ± 0.02, are shown in Fig. 2a. Dissolution rates were determined from the slope of the normalized weight loss versus time plot over the course of the experiment, and these rates decreased by several orders of magnitude with increasing alumina content. For example, the dissolution rates for the glasses shown in Fig. 2a decreased from 2.5×10^{-5} g/cm^2-min for the 50.9ZnO–6.1Al_2O_3–43.0P_2O_5 glass (O/P = 3.30) to $<3 \times 10^{-8}$ g/cm^2-min for the 28.3ZnO–19.9Al_2O_3–51.8P_2O_5 glass (O/P = 3.35), as shown in Fig. 2b. Similar decreases in dissolution rates were noted for alumina additions in other series of glasses with similar O/P ratios. For example, the dissolution rates for ZAP glasses with average O/P ratio of 3.06 ± 0.03 are also shown in Fig. 2b.

Table 2 gives the properties of the ZAP glasses. For glasses with similar O/P ratios, the densities decrease systematically with greater Al_2O_3, as shown for two series in Fig. 3a. The densities of glasses with low alumina contents (<2.5 mol%) are similar to the densities of binary Zn-phosphate glasses reported in the literature [20,45,46]. The overall effects of composition on density are summarized in the contour plot in Fig. 3b. In addition to the systematic decrease in density with increasing alumina content, there is a significant increase in density with

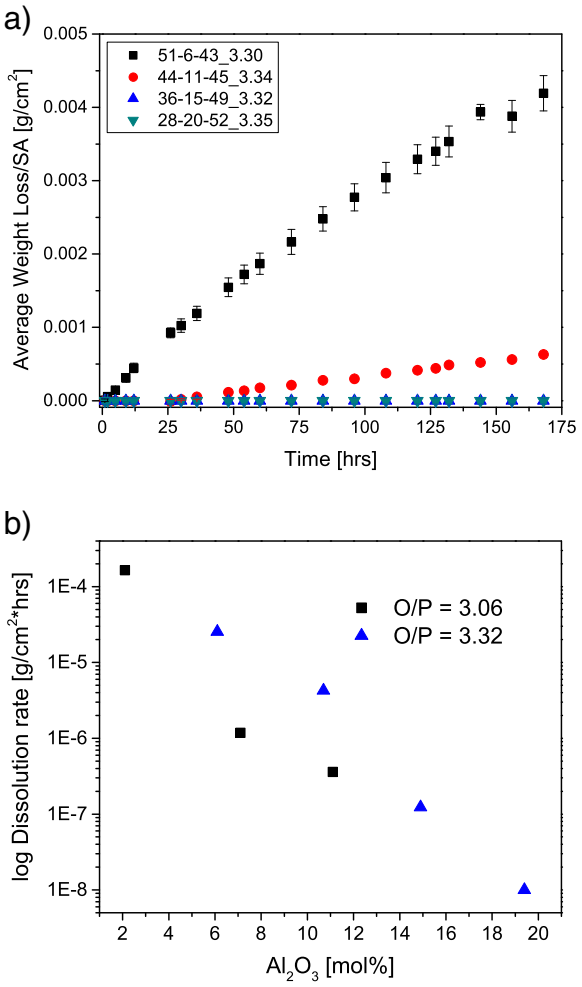

Fig. 2. a. Weight loss data and b. log dissolution rates for ZAP glasses with O/P ratio = 3.06 ± 0.03 and 3.32 ± 0.02, in deionized water at room temperature.

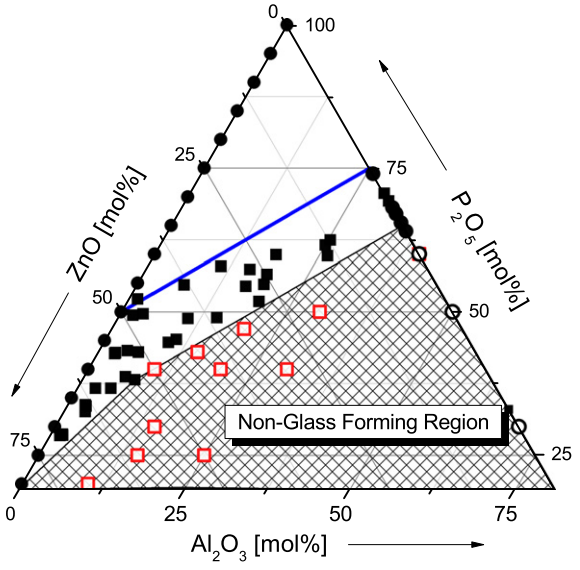

Fig. 1. ZAP compositional diagram. Compositions of melt-quenched glasses are shown as black squares and compositions that were un-melted (1500 °C) or crystallized on quenching are indicated by open squares. The cross-hatched area represents the non-glass forming range. The compositions of melt quenched glasses reported in the literature [17,20,26,41,43] are shown as black circles and those reported to be non-glass forming compositions are shown as open circles The blue line indicates where: O/P = 3 with increasing alumina from left to right.

Table 2
Properties of the ZnO–Al_2O_3–P_2O_5 glasses.

Glass designation[a]	Density [g/cm^3]	T_g [°C]	CTE [°C^{-1}] (×10^{-6})	Refractive index
46-2-52_2.99	2.759	nm	nm	nm
49-2-49_3.05	2.899	450	6.5	1.5268
47-3-50_3.08	2.779	436	nm	1.5238
38-7-55_3.04	2.778	515	6.2	1.5219
33-11-56_3.10	2.736	525	6.3	1.5226
27-16-57_3.15	2.691	606	nm	1.5238
22-18-60_3.14	2.649	611	nm	1.5218
0-29-71_3.12	2.578	753	5.6	1.5284
55-3-43_3.23	3.033	433	6.2	1.5450
52-4-43_3.26	2.919	437	6.1	1.5325
40-11-49_3.24	2.855	449	5.3	1.5250
25-19-57_3.22	2.631	560	nm	1.5133
26-19-55_3.26	2.666	582	5.9	1.5184
13-25-62_3.22	2.571	633	5.6	1.5134
0-34-66_3.27	2.489	795	nm	1.5105
51-6-43_3.30	2.996	442	5.8	1.5446
44-11-45_3.34	2.811	452	5.3	1.5213
36-15-49_3.32	2.667	492	5.1	1.5086
28-20-52_3.35	2.573	533	nm	1.5033
61-3-37_3.44	3.321	441	6.8	1.5729
58-5-37_3.50	3.291	445	6.4	1.5767
55-6-39_3.45	2.995	465	nm	1.5426
63-3-34_3.56	3.552	453	6.6	1.6115
64-4-33_3.63	3.418	nm	nm	1.5946
70-2-29_3.81	3.736	462	nm	1.6323

[a] In mol%, ZnO–Al_2O_3–P_2O_5_O/P ratio.

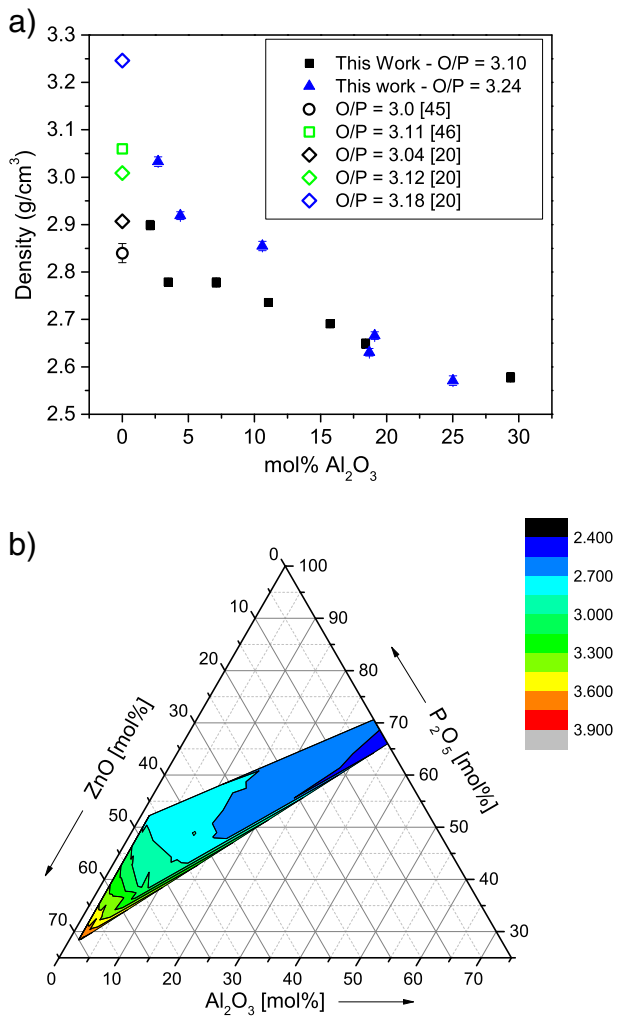

Fig. 3. Density for glasses in the ZAP system a. with varying alumina content and the indicated O/P ratios, with representative densities from the literature (open symbols); b. as a contour plot for all compositions.

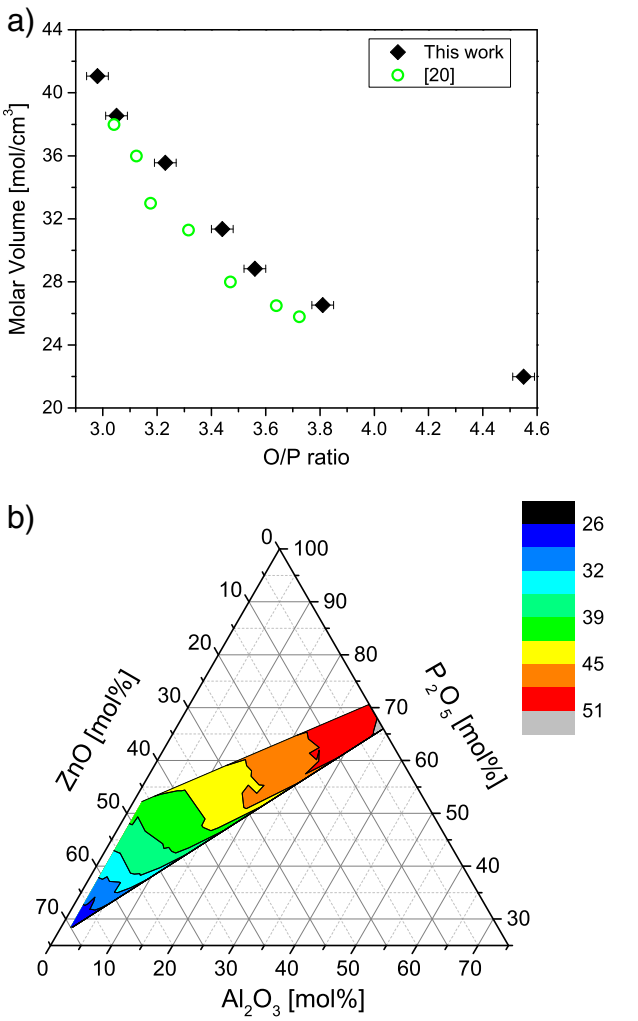

Fig. 4. Molar volume for glasses in the ZAP system a. with constant Al_2O_3 content (2.1 ± 0.7 mol%) and varying O/P ratio from this work (black) and from Brow et al. [20]. (open green circles) and b. as a contour plot for all compositions.

increasing ZnO content, particularly for glasses with low alumina-contents. Fig. 4 shows that the molar volume of ZAP glasses with low (<2.5 mol%) Al_2O_3-contents decreases systematically with increasing ZnO content, again in agreement with an earlier study of binary Zn-phosphate glasses [20]. The ZAP glasses have slightly greater molar volumes than the binary ZP glasses because the small amounts of alumina in the former reduce density relative to the latter (Fig. 3b). The overall relationship between molar volume and ZAP glass composition is shown in the contour plot in Fig. 4b.

Fig. 5a shows the effect of alumina content on the glass transition temperature (T_g) for two series of ZAP glasses with O/P ratios of 3.10 and 3.24. The inset shows T_g for glasses with similar Al_2O_3 contents (~2.7 mol% and ~10 mol%) as a function of Zn/P ratio. There is a minimum in T_g for a Zn/P ratio close to 0.75. The overall compositional trends can be more easily seen in the contour plot shown in Fig. 5b.

The coefficient of thermal expansion (CTE) of the ZAP glasses is in the range of 5–7 × 10^{-6}/°C, and decreases with increasing alumina contents (Table 2).

The effects of the ZnO content on the refractive index (at 632.8 nm) for glasses with low (~2.4 mol%) alumina contents are shown in Fig. 6a, and the overall effects of composition are shown in the contour plot in Fig. 6b. It is clear that the ZnO content has the most significant effect on refractive index; viz., Fig. 6a.

3.2. Structural characterization

Fig. 7 shows the Raman spectra of glasses with similar O/P ratios (3.23 ± 0.02) and increasing Al_2O_3 contents. The spectra from glasses with ~2 mol% Al_2O_3 in this work are similar to spectra reported elsewhere for binary Zn-phosphate glasses [20,26,47], and peak assignments from those studies are used here (Table 3). For the spectra in Fig. 7, the peaks near 700 cm^{-1} are assigned to the symmetric stretch of bridging oxygens in Q^2 units and there is a shoulder near 750 cm^{-1} in some of these spectra that is assigned to P–O–P stretching modes associated with chain terminating (Q^1) tetrahedra. The intense peak near 1200 cm^{-1} and the shoulder near 1250 cm^{-1} are assigned, respectively, to the PO_2 symmetric and asymmetric stretching modes of non-bridging oxygens associated with Q^2 units. Peaks associated with both the P–O–P and PO_2 stretching modes become broader and shift to greater frequencies with increasing alumina contents. In addition, a shoulder to the PO_2 peak near 1100 cm^{-1} develops with increasing alumina and this may be related to the presence of chain terminating Q^1 sites, the PO_3 stretching mode listed in Table 3.

^{31}P MAS NMR spectra are shown in Fig. 8a and b for select glasses with similar O/P ratios (3.09 ± 0.05) and with similar alumina contents (2–3 mol%) but varying O/P ratios, respectively. The peaks near −31 ppm in Fig. 8a are associated with Q^2 units and the small peak near

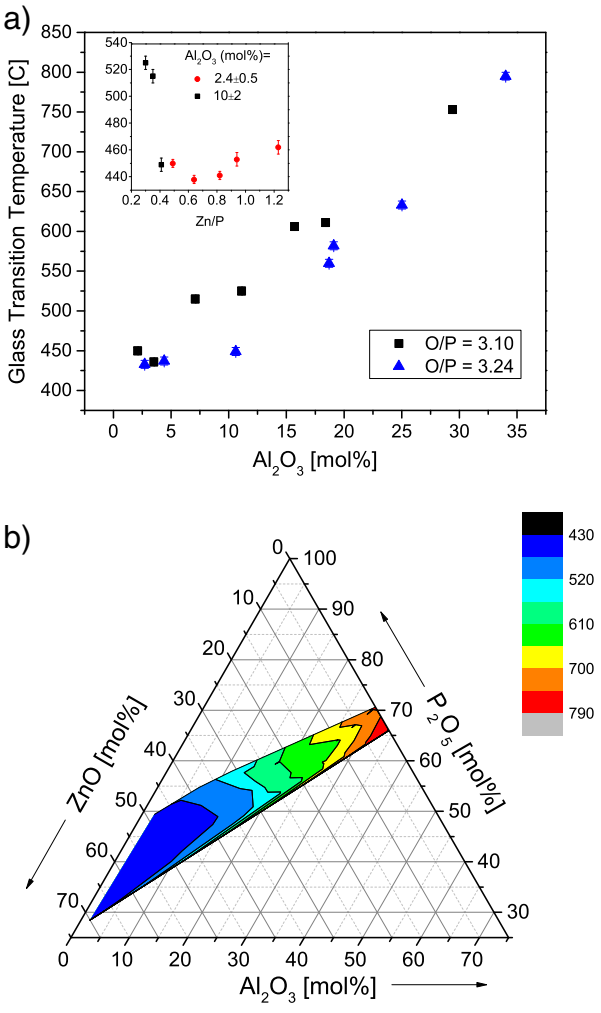

Fig. 5. Glass transition temperature for glasses in the ZAP system as a function of Al_2O_3 content for the indicated O/P ratio (Inset: Tg vs. Zn/P ratios for the indicated alumina contents) and b. as a contour plot for all compositions.

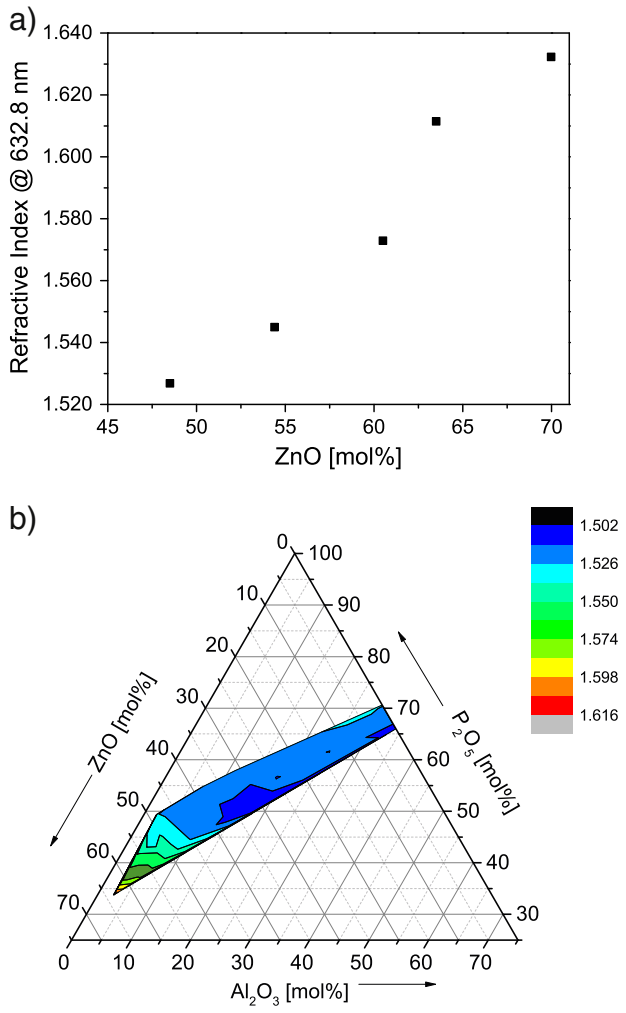

Fig. 6. Refractive index for glasses in the ZAP system a. for a constant Al_2O_3 content (2.4 ± 0.5 mol%) and increasing ZnO content; and b. as a contour plot for all compositions.

−10 ppm is due to Q^1 tetrahedra [20]. The Q^2 peak systematically broadens and shifts to more negative ppm for glasses with increasing alumina content; similar behavior has been reported for Q^2 ^{31}P peaks from other aluminophosphate glasses with similar O/P ratios [35,37,48]. The shift and broadening of this ^{31}P resonance is due to the formation of P–O–Al bonds, which modify the chemical shielding of the Q^2 sites. Fig. 8b shows how changing the O/P ratio affects the principal peaks and their associated spinning sidebands. As the O/P ratio increases, peaks due to Q^2 tetrahedra (near −31 ppm) are replaced by those due to Q^1 tetrahedra (−13 ppm) and Q^0 tetrahedra (+3 ppm), in agreement with previous studies [20].

Fig. 9a shows the ^{27}Al NMR spectra for glasses with similar O/P ratios (3.09 ± 0.04) and with increasing alumina content. There are three distinct peaks in these spectra, each indicating a different coordination environment for aluminum. The peaks are centered near 36 ppm, 7 ppm and −17 ppm and are attributed to 4-, 5-, and 6-coordinated aluminum, respectively [35,49,50]. As more alumina is added to the glasses with similar O/P ratios, the average aluminum coordination number, calculated from the respective areas of each peak, increases as shown in Fig. 9b.

Fig. 10a shows the HPLC chromatographs of glasses with similar Al_2O_3 contents (2–3 mol%) and different O/P ratios, whereas Fig. 10b shows chromatographs of glasses with similar O/P ratios (3.33 ± 0.02) and increasing alumina contents. Each peak represents a P-anion with increasing numbers of tetrahedra (left-to-right). These phosphate anions are described using the P_n terminology where n is the number of P-tetrahedra in a chain. Glasses with low O/P ratios (close to 3.0) possess longer chains, which are unresolved by the HPLC method and these longer chains form the large hump at longer retention times, as seen in Fig. 10a. The chromatograph from the glass with the largest O/P ratio in Fig. 10a (O/P = 3.56) is dominated by

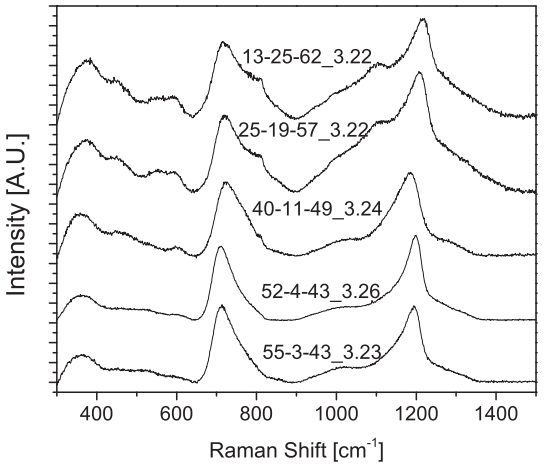

Fig. 7. Raman spectra of ZAP glasses with similar O/P ratios (3.23 ± 0.02) and increasing Al_2O_3 contents.

Table 3
Raman peak assignments from the literature.

Wavenumber (cm^{-1})	Structural units	Reference	Wavenumber (cm^{-1})	Structural units	Reference
~350	Bending mode of phosphate polyhedral with zinc modifier	[20]	950–970	$(PO_4)_{symm}$ stretch (NBO), Q^0s	[18,20]
~575	Bend mode related to zinc phosphate network or ZnO_4	[18,20]	1010	P–O stretch, Q^1 chain terminator	[20,47]
680	Symm vibrations of P–O–P bonds	[18, 60]	1048	$(PO_3)_{symm}$ stretch (NBO), Q^1s	[20,47]
702	POP_{symm} stretch (BO), Q^2s	[18,20,47]	1138 (40)	P–O stretch, Q^1 chain terminator	[18,20,47]
750	Symm vibrations of P–O–P BO atoms	[61]	1170–1180	Stretching vibrations of O–P–O/Symm vibrations of middle chain units (PO_2)	[60, 61]
758	POP_{symm} stretch (BO), Q^1s	[20,47]	1150–1210	$(PO_2)_{symm}$ stretch (NBO), Q^2s	[18,20,47]
790	$(P–O–P)_s$ stretch in very short phosphate chains or in rings	[18]	1210–1260	$(PO_2)_{asymm}$ stretch (NBO), Q^2s	[18,20,47]
930	Asymmetric vibrations of P–O–P	[61]			

peaks associated with P_1 (29% relative area), P_2 (52%) and P_3 (15%) anions. The chromatographs for the glasses with similar O/P ratios and increasing alumina contents (Fig. 10b) are similar, but possess slightly broader anion distributions for glasses with greater alumina contents.

4. Discussion

The addition of alumina to zinc phosphate glass significantly improves the chemical durability (Fig. 2); making it possible to design more chemically stable optical substrates for writing optical elements with femto-second lasers. Recent research at UC-Davis [51] has shown that optical waveguides can be written into the more durable ZAP glasses with O/P ratios near 3.25 and that the characteristics of these waveguides are as good, or better, as those written into less durable, alumina-free glasses [7,52].

The density and refractive index of the ZAP glasses are most dependent on the ZnO-content. Glasses with greater ZnO-contents have greater densities (Fig. 3) due in part to the greater relative mass of Zn, compared to Al and P, and to the lower molar volumes of the ZnO-rich glasses (Fig. 4). The refractive indices of the ZnO-rich glasses are also greater. This is consistent with both the greater ionic refractivity of Zn^{2+} (0.7), compared to Al^{3+} (0.14) and P^{5+} (0.05) [53], and the expected greater refractivity of oxygens associated with the P–O–Zn bonds as compared with oxygens in P–O–P and P–O–Al bonds [54]. For glasses with similar ZnO-contents, the replacement of P_2O_5 by Al_2O_3 has little effect on either density or refractive index.

4.1. Phosphate anion distributions

When less-acidic metal oxides are combined with P_2O_5 in a melt, the metal oxide polyhedra are incorporated into the phosphate network by sharing oxygens with the phosphate anions. For the ZAP glasses, these structural changes can be summarized by the following reactions:

$$P–O–P + ZnO \rightarrow P–O–Zn–O–P \quad (3)$$

$$P–O–P + Al_{2/3}O \rightarrow P–O–Al_{2/3}–O–P. \quad (4)$$

The net effect of reactions that reduce the relative numbers of bridging oxygens (P–O–P), like those shown above, is a reduction in the average size of the polyphosphate anions. If one considers a metaphosphate glass (O/P = 3) as consisting of Q^2 tetrahedra that form long chain, or ring, anions then the addition of ZnO and/or Al_2O_3 will shorten those chains (or replace the rings) by incorporating the additional oxygen into chain-terminating (Q^1) sites. Evidence for such structural modifications of glasses with increasing O/P ratios can be readily seen in the Raman and ^{31}P NMR spectra, and in the chromatographic data. For example, the Q^2 peak near −31 ppm in the ^{31}P NMR spectra in Fig. 8b is dominant for the glass with O/P = 3.05, but becomes a shoulder on the dominant Q^1 peak at −13 ppm for the glass with O/P = 3.44. The further incorporation of ZnO to increase O/P to 3.56 results in the creation of Q^0 sites (+3 ppm) to accommodate the added oxygen.

The chromatographic data shown in Fig. 10a indicates that the phosphate anions become progressively shorter with increasing O/P ratio. The large hump at longer retention times, due to unresolvable anions with more than about 13 P-tetrahedra, for the glass with an O/P = 3.05 is replaced by single peaks due to anions with four or fewer P-tetrahedra for the glass with an O/P = 3.56. The relationship between the incorporation of oxygen (increasing O/P ratio) into the phosphate network with the addition of metal oxide (whether ZnO or Al_2O_3) and the average phosphate anion can be quantitatively described

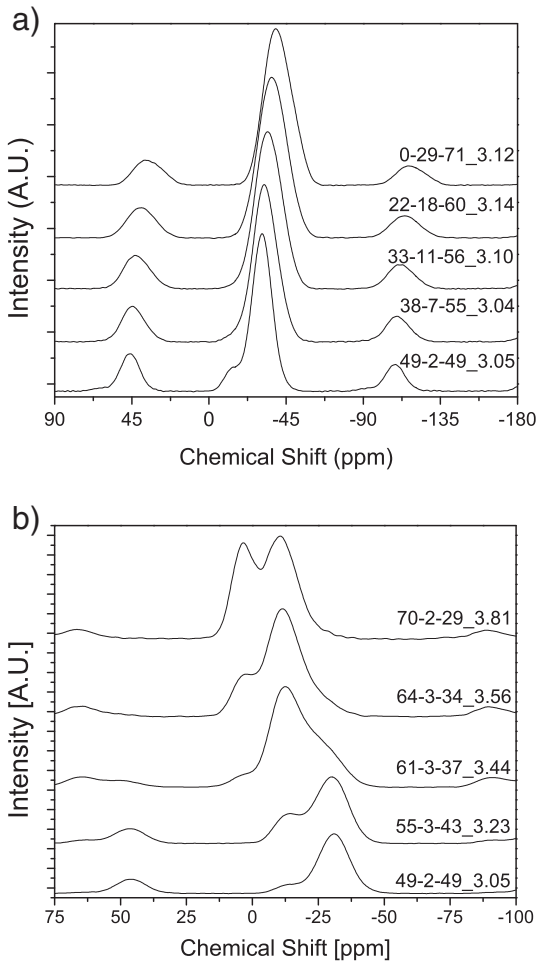

Fig. 8. ^{31}P NMR spectra of ZAP glasses with a. similar O/P ratios (3.09 ± 0.04) and increasing Al_2O_3 contents; and b. similar Al_2O_3 contents (2.4 ± 0.5 mol%) and increasing O/P ratios.

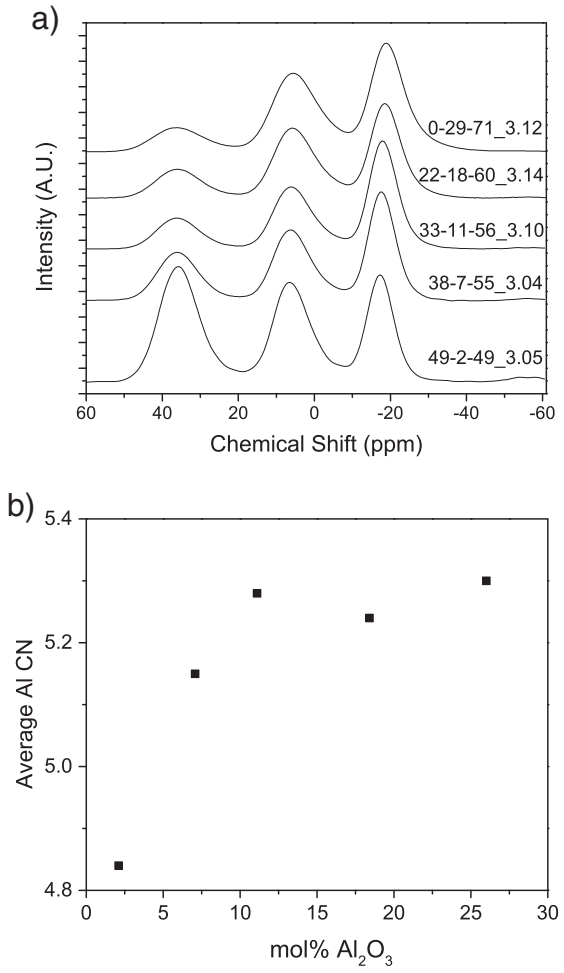

Fig. 9. a. ^{27}Al MAS NMR spectra from ZAP glasses with similar O/P ratios (3.09 ± 0.04) and b. a plot of the average Al CN as obtained from the ^{27}Al MAS NMR spectra.

[44]. For a glass with the nominal composition $xM_{2/v}O\ (1-x)P_2O_5$, the average phosphate anion chain-length, $\overline{n}$, will be given by

$$\overline{n} = \frac{2}{\sum_j \frac{[M_j][v_j]}{[P]} - 1} \tag{5}$$

where v is the valence of the metal oxide and $[M_j]$ and [P] are the relative atomic fractions of the metal ions and phosphorus, respectively [24]. Using the compositions of the ZAP glasses (Table 1), the predicted $\overline{n}$ from Eq. (5) can be compared with that obtained from their respective chromatographs; that comparison is shown in Fig. 11. The average chain lengths can also be obtained from the ^{31}P NMR spectra through peak fitting and using the relative percentages of the Q^n units with the following equation:

$$\overline{n} = \left(\frac{100}{\left[\%Q^1 \Big/ 2 \right] + \%Q^0} \right). \tag{6}$$

The close agreement between the predicted and measured average chain lengths (Fig. 11) across the entire range of compositions (O/P ratios) indicates that both ZnO and Al_2O_3 have similar effects on the development of the phosphate network and that reactions (3) and (4) adequately summarize those effects.

For samples with a fixed O/P ratio, the average chain length should be constant. For example, the glasses in Fig. 10b each have an O/P ratio of about 3.33 and, by using Eq. (5), have an average chain length of 3.0 (±0.2) tetrahedra. However, the chromatographs indicate that the chain length distribution becomes slightly broader with increasing alumina content. Al_2O_3 has also been noted to promote the disproportionation of pyrophosphate anions in the glass melt, as described by [44]

$$2P_2 \rightarrow P_1 + P_3. \tag{7}$$

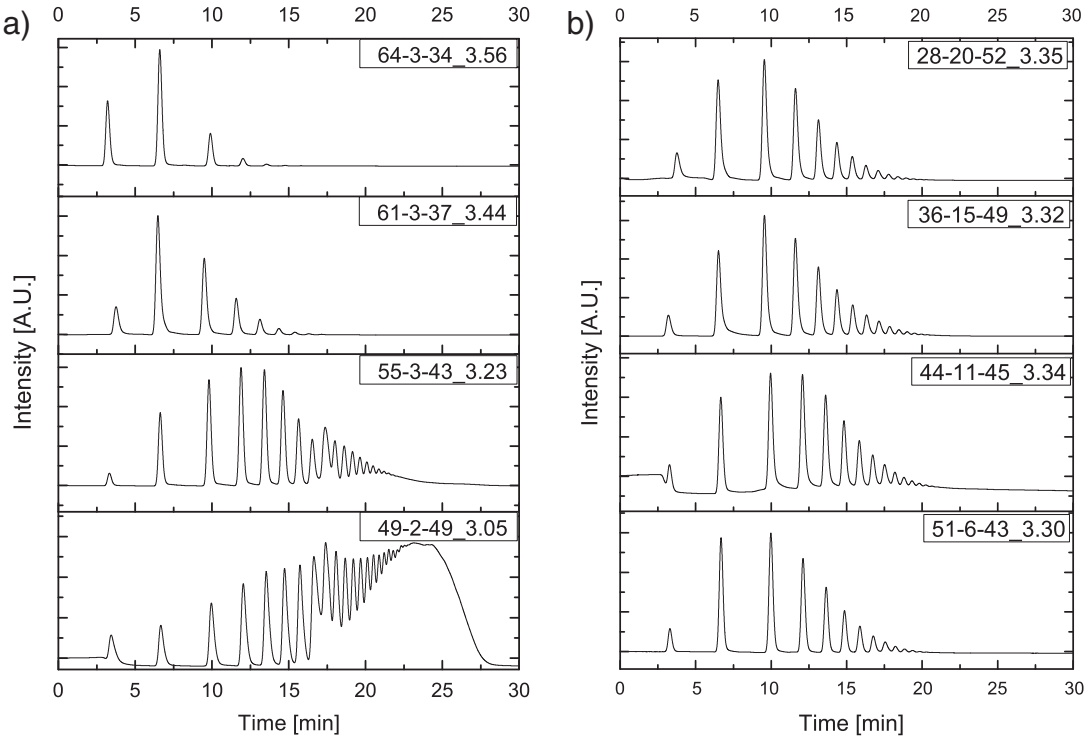

Fig. 10. HPLC spectra of ZAP glasses with a. constant Al_2O_3 (2.6 ± 0.3 mol%) and different O/P ratios; and b. glasses with similar O/P ratios (3.33 ± 0.2) and different Al_2O_3 contents.

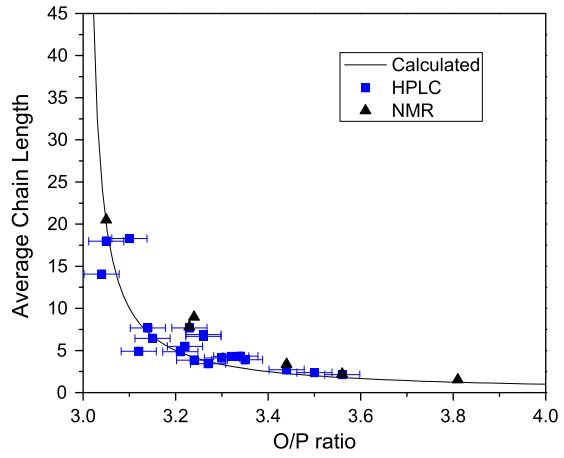

Fig. 11. Plot of the average chain length measured from the HPLC chromatographs (blue) and NMR spectra (black) against the O/P ratios from analyzed compositions of the ZAP glasses. The solid line is the expected relationship, based on Eq. (5).

If this reaction can be described in terms of a chemical equilibrium, then the reaction constant (k_2) will be determined from [44]:

$$k_2 = \frac{[P_3] \times [P_1]}{[P_2]^2} \quad (8)$$

where $[P_n]$ is the area under the nth peak from the HPLC chromatograms.

Fig. 12 shows that k_2 increases with increasing alumina-content for two series of glasses with similar O/P ratios. Thus, the replacement of ZnO by Al_2O_3 broadens the distribution of P-anions that constitute the glass structure.

The replacement of ZnO by Al_2O_3 also affects the average properties of the P–O bonds associated with the different metal polyhedra. For example, Fig. 13a shows the effect of the relative concentration of Al_2O_3 on the Raman peak position of the PO_2 stretching mode for a series of ZAP glasses with similar O/P ratios, and Fig. 13b shows the position of the ^{31}P NMR peak for the Q^2 tetrahedra for the same glasses. In both cases, there are systematic changes in the peak positions as Al replaces Zn: the PO_2 Raman peak increases in frequency and the ^{31}P NMR Q^2 peak shifts to more negative ppm. Both of these spectral trends indicate a general strengthening, or shortening, of the average P–O bonds associated with the different metal polyhedra. For example, Nelson et al. [55] showed that as the bond force of the metal cation on

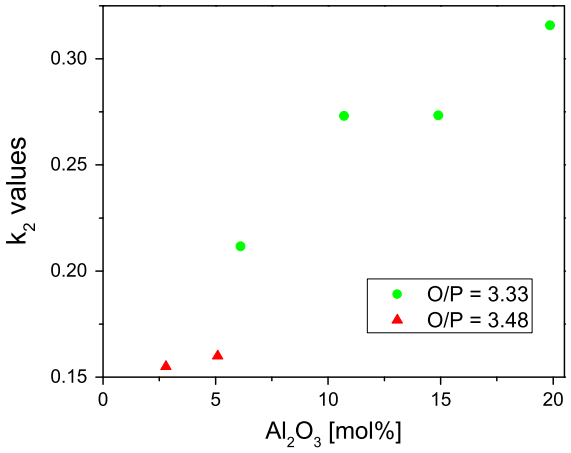

Fig. 12. k_2 values calculated from HPLC chromatographs for ZAP glasses with O/P ratios = 3.33 (±0.02) and 3.47 (±0.04).

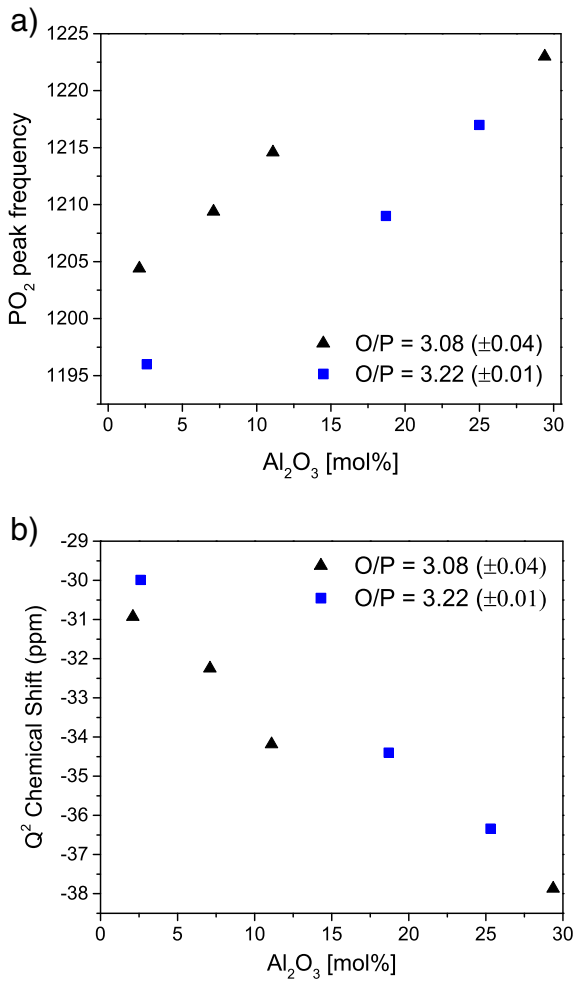

Fig. 13. a. PO_2 Raman frequency change and b. Q^2 chemical shift as a function of alumina content for select glasses.

the PO_2 vibrational unit increases there is a shift to greater frequency of the associated peaks. Popovic et al. have also shown that positive shifts in Raman frequencies result from the systematic shortening of P–O bonds [56]. Similar explanations have been offered for the compositional effects on the positions of ^{31}P NMR peaks in aluminophosphate glasses. For example, it has been shown that the ^{31}P peak for a Q^2 unit connected to an alkali or alkaline earth ion will occur at a more positive chemical shift than the ^{31}P peak for a Q^2 unit connected to aluminum [35]. The chemical shifts of phosphorus become more negative, representing a less shielded P nucleus, with the increase in the cationic potential (charge/radius) for the metal oxides. This is due to the increased MO covalency depleting electron density on the phosphorus, leading to decreased shielding.

The replacement of ZnO by Al_2O_3 substantially increases the glass transition temperature (Fig. 5a and b) and decreases the coefficient of thermal expansion (Table 2). Similar property trends are noted for other phosphate glasses (i.e., Na-aluminophosphate glasses [35]) and can be related to the replacement of Zn–O–P bonds by stronger Al–O–P bonds to link neighboring phosphate anions. These stronger bonds are associated with both a greater field strength metal cation ($FS_{Al3+} > FS_{Zn2+}$) and the stronger, shorter P–O bonds implied by shifts in the Raman and ^{31}P NMR peaks.

4.2. Al-coordination environments

The nature of the coordination polyhedra of the Zn^{2+} and Al^{3+} ions is expected to influence the glass properties. For example, breaks in the

compositional trends of properties like T_g, density and refractive index for Na-aluminophosphate (NAP) glasses were related to changes in the average Al coordination number [35]. Although CN_{Al} changes systematically with composition for the ZAP glasses (i.e., Fig. 9), the compositional dependence of CN_{Al} for these glasses differs from what is seen with the NAP glasses. For NAP glasses with O/P ratios near 3.0, octahedral Al dominates the aluminophosphate structures. In contrast, the average coordination number of Al in the ZAP glasses with O/P $\approx$3.08 is under 5, and it increases as Al_2O_3 replaces ZnO (Fig. 9b). For the NAP glasses, the average CN_{Al} depends on the charge associated with the P-anion [35]. A different relationship exists between CN_{Al} and the compositions of the ZAP glasses.

Hoppe has shown that the coordination environment of a metal cation incorporated in a phosphate glass is influenced by the number of terminal (nonbridging) oxygens (TO) available to coordinate that metal cation [57]. For binary phosphate glasses with the molar composition $xM_{2/\nu}O\ (1-x)P_2O_5$, where ν is the valence on the metal cation (M), the number of terminal oxygens per M is given by

$$N_{TO} = \nu(x+1)/x. \quad (9)$$

Hoppe noted that when N_{TO} was greater than the coordination number of the $M^{\nu+}$ cation (CN_M), then those cation polyhedra could be incorporated into a phosphate structure without needing to share terminal oxygens with other metal cation polyhedra. When N_{TO} was less than CN_M, then some of the cation polyhedra must share TO. The compositional dependence of the properties of many binary phosphate glasses changes at compositions where $N_{TO} = CN_M$ [57], and in other systems [28], CN_M decreases with increasing $R_{2/\nu}O$ content so that the cation polyhedra avoid sharing common terminal oxygens. Indeed, Brow et al. [42] have shown that the average coordination number of Al-polyhedra in binary aluminophosphate glasses follows Eq. (9), decreasing with increasing O/P ratio to prevent Al-polyhedra from sharing common TO.

Hoppe's model can be extended to ternary glasses to explain the effects of composition on the CN_{Al} in the ZAP glasses. Consider first the coordination number of the Zn-ions. It has been shown in X-ray and neutron diffraction studies of binary zinc phosphate glasses [21,23,58] that the preferred coordination number for Zn is four. If one assumes that $CN_{Zn} = 4$ for the ZAP glasses and that these Zn tetrahedra do not share terminal oxygens with each other or with any Al-polyhedra, then the number of terminal oxygens remaining, per Al, can be calculated from the molar fractions of the glass constituents according to:

$$\frac{TO}{Al} = \frac{(6[Al_2O_3] + 2[P_2O_5] - 2[ZnO])}{2[Al_2O_3]}. \quad (10)$$

Following Hoppe, the ratio TO/Al should then be the minimum CN_{Al} to prevent Zn-tetrahedra and/or Al-polyhedra from sharing common terminal oxygens on any phosphate anions, and for every terminal oxygen to link to one ZnO_4 or one AlO_x polyhedron, where x = 4, 5, or 6. If TO/Al < 4.0, then some metal cation polyhedra must share common terminal oxygens.

Fig. 14 compares the TO/Al ratio from Eq. (10) with the average CN_{Al} determined from the ^{27}Al NMR spectra for the ZAP glasses, as well as for several Mg-aluminophosphate (MAP) glasses described in the literature [59]. The ion sizes of Mg^{2+} and Zn^{2+} are similar so it is likely that Mg-tetrahedra are present in the structures of the MAP glasses and a similar analysis of CN_{Al} can then be made for those compositions. Also shown in Fig. 14 are the CN_{Al} reported in an NMR study of binary aluminophosphate (AP) glasses [42] and calculated from Eq. (10). There is good agreement between CN_{Al} determined from the ^{27}Al NMR spectra of the ZAP, MAP, and AP glasses for TO/Al > 4 and the CN_{Al} calculated from Eq. (10). This agreement indicates that the coordination environment of the Al-polyhedra is determined by the number of available terminal oxygens and adjusts to avoid sharing common TOs with the Zn- (or Mg-) tetrahedra that also link different phosphate anions. When TO/Al < 4, then some terminal oxygens must be shared by neighboring Al- and/or Zn-polyhedra, and Eq. (10) can no longer be used to predict CN_{Al}.

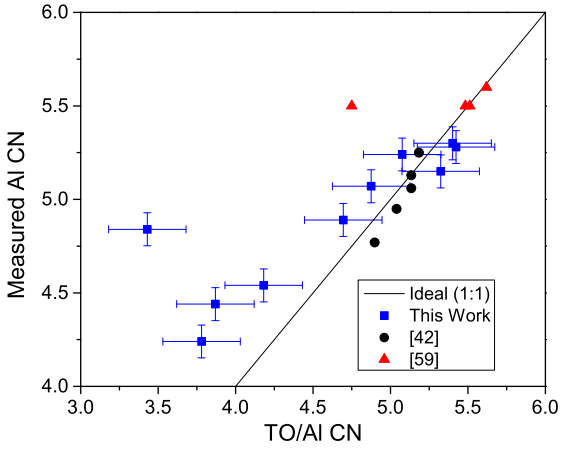

Fig. 14. Average Al-coordination number plotted against the TO/Al ratio for ZAP glasses from this work (blue), and for MAP glasses [59] and binary aluminophosphate glasses [42] reported in the literature. The expected relationship for TO/Al > 4 (from Eq. (10)) is given as the solid line.

5. Conclusions

An investigation of the properties and structures of zinc aluminophosphate glasses has been completed. The corrosion rate in water has been found to decrease by orders of magnitude with the addition of alumina. For glasses with a constant O/P ratio, increasing amounts of alumina increases the T_g, molar volume and refractive index, while decreasing the density and coefficient of thermal expansion. Spectroscopic and chromatographic measurements reveal that the addition of both zinc and aluminum oxide disrupts the phosphate network, creating smaller phosphorus–oxygen anions. Increasing the alumina content results in shorter, stronger P – O bonds in the network and enhances the disproportionation of phosphate anions at higher O/P ratios.

The coordination number of aluminum depends on the number of terminal oxygens available in the network and the avoidance of metal polyhedra that share common oxygens on a P-tetrahedron. The compositional dependence of CN_{Al} is consistent with Hoppe's model of modifier coordination in phosphate glasses.

Acknowledgments

The authors acknowledge the Department of Education for the Graduate Assistance in Areas of National Need (GAANN) fellowship and the National Science Foundation (DMR 1207520) for funding this work. The authors are also grateful to the FEDER, Region Nord Pas-de-Calais, Ministère de l'Education Nationale de l'Enseignement Superieur et de la Recherche, CNRS, and USTL for the funding of NMR spectrometers. The contributions of Missouri S&T colleagues Dr. Jen-Hsien Hsu for the EDS compositional analysis, Lina Ma for helpful discussions, and Ryan Jones for assistance with the synthesis and characterization of the ZAP glasses are greatly appreciated, as are the discussions on femto-second laser processing with Prof. Denise Krol and her colleagues at UC-Davis.

References

[1] B.G. Aitken, D.C. Bookbinder, M.E. Green, R.M. Morena, Non-lead sealing glasses (Patent US5246890 A), in. Corning Incorporated, United States, 1993.
[2] R.M. Morena, Phosphate glasses as alternatives to Pb-based sealing frits, J. Non-Cryst. Solids 263&264 (2000) 6.

[3] J.A. Wilder Jr., Glasses and glass ceramics for sealing to aluminum alloys, J. Non-Cryst. Solids 38&39 (1980) 6.
[4] R. Martinez-Martinez, A. Speghini, M. Bettinelli, C. Falcony, U. Caldino, White light generation through the zinc metaphosphate glass activated by Ce^{3+}, Tb^{3+} and Mn^{2+} ions, J. Lumin. 129 (2009) 5.
[5] C.T. Lin, S.W. Yung, J. Lin, W.S. Chen, C.H. Lai, Y.M. Lee, J.S. Lin, Luminescence properties of Tm^{3+}/Dy^{3+} co-doped zinc–aluminum phosphate glasses for white LED, Adv. Mater. Res. 602–604 (2013) 9.
[6] A. Eriah, S.G. Bhat, Optical properties of samarium doped zinc-phosphate glasses, J. Phys. Chem. Solids 68 (2007) 5.
[7] L.B. Fletcher, J.J. Witcher, N. Troy, S.T. Reis, R.K. Brow, R.M. Vazquez, R. Osellame, D.M. Krol, Femtosecond laser writing of waveguides in zinc phosphate glasses, Opt. Mater. Express 1 (2011) 845–855.
[8] L.B. Fletcher, J.J. Witcher, N. Troy, R.K. Brow, D.M. Krol, Single-pass waveguide amplifiers in Er–Yb doped zinc polyphosphate glass fabricated with femtosecond laser pulses, Opt. Lett. 37 (7) (2012) 3.
[9] N. Troy, L.B. Fletcher, S.T. Reis, R.K. Brow, H. Huang, L. Yang, J. Liu, D.M. Krol, Structural modification in Er–Yb doped zinc phosphate glasses with megahertz repetition rate femtosecond pulses, in: T. I. S. f. O. Engineering (Ed.), Frontiers in Ultrafast Optics: Biomedical, Scientific, and Industrial Applications XII, vol. 8247, The International Society for Optical Engineering, San Francisco, CA, 2012.
[10] L.B. Fletcher, J.J. Witcher, N. Troy, S.T. Reis, R.K. Brow, Effects of rare-earth doping on femtosecond laser waveguide writing in zinc polyphosphate glass, J. Appl. Phys. (2012) 112.
[11] L.B. Fletcher, J.J. Witcher, N. Troy, S.T. Reis, R.K. Brow, D.M. Krol, Direct femtosecond laser waveguide writing inside zinc phosphate glass, Opt. Express 19 (9) (2011).
[12] L. Canioni, M. Bellec, A. Royon, B. Bousquet, T. Cardinal, Three-dimensional optical data storage using third-harmonic generation in silver zinc phosphate glass, Opt. Lett. 33 (4) (2008) 3.
[13] E. Kordes, Z. Phys. Chem. 50B (1941) 194.
[14] E. Kordes, R. Nieder, Glastechn. Ber. 41 (1968).
[15] E. Kordes, W. Vogel, R. Feterowsky, Z. Elektrochem. 57 (1953) 282.
[16] M. Crobu, A. Rossi, F. Mangolini, N.D. Spencer, Chain-length-identification strategy in zinc polyphosphate glasses by means of XPS and ToF-SIMS, Anal. Bioanal. Chem. 403 (2012) 8.
[17] K. Meyer, Characterization of the structure of binary zinc ultraphosphate glasses by infrared and Raman spectroscopy, J. Non-Cryst. Solids 209 (1997) 227–239.
[18] J. Schwarz, H. Ticha, L. Tichy, R. Mertens, Physical properties of PbO–ZnO–P_2O_5 glasses. I. Infrared and Raman spectra, J. Optoelectron. Adv. Mater. 6 (3) (2004) 737–746.
[19] R.K. Brow, Review: the structure of simple phosphate glasses, J. Non-Cryst. Solids 263&264 (2000) 1–28.
[20] R.K. Brow, D.R. Tallant, S.T. Meyers, C.C. Phifer, The short-range structure of zinc polyphosphate glass, J. Non-Cryst. Solids 191 (1995) 45–55.
[21] E. Matsubara, Y. Waseda, M. Ashizuka, E. Ishida, Structural study of binary phosphate glasses with MgO, ZnO, and CaO by X-ray diffraction, J. Non-Cryst. Solids 103 (1988) 8.
[22] K. Suzuya, K. Itoh, A. Kajinami, C.K. Loong, The structure of binary zinc phosphate glasses, J. Non-Cryst. Solids 345&346 (2004) 80–87.
[23] G. Walter, U. Hoppe, J. Vogel, G. Carl, P. Hartmann, The structure of zinc polyphosphate glass studied by diffraction methods and ^{31}P NMR, J. Non-Cryst. Solids 333 (2004) 11.
[24] B.C. Sales, J.U. Otaigbe, G.H. Beall, L.A. Boatner, J.O. Ramey, Structure of zinc polyphosphate glasses, J. Non-Cryst. Solids 226 (1998) 287–293.
[25] J.W. Wiench, B. Tischendorf, J.U. Otaigbe, M. Pruski, Structure of zinc polyphosphate glasses studied by two-dimensional solid and liquid state NMR, J. Mol. Struct. 602–603 (2002) 13.
[26] B. Tischendorf, J.U. Otaigbe, J.W. Wiench, M. Pruski, B.C. Sales, A study of short and intermediate range order in zinc phosphate glasses, J. Non-Cryst. Solids 282 (2001) 147–158.
[27] R.K. Brow, An XPS study of oxygen bonding in zinc phosphate and zinc borophosphate glasses, J. Non-Cryst. Solids 194 (1996) 267–273.
[28] U. Hoppe, R.K. Brow, D. Ilieva, P. Jovari, A.C. Hannon, Structure of rare-earth phosphate glasses by X-ray and neutron diffraction, J. Non-Cryst. Solids 351 (2005) 12.
[29] H. Takebe, Y. Baba, M. Kuwabara, Dissolution behavior of ZnO–P_2O_5 glasses in water, J. Non-Cryst. Solids 352 (2006) 3088–3094.
[30] L. Koudelka, P. Mosner, Study of the structure and properties of Pb–Zn borophosphate glasses, J. Non-Cryst. Solids 293–295 (2001) 7.
[31] S. Chenu, U. Werner-Zwanziger, C. Calahoo, J.W. Zwansiger, Structure and properties of $NaPO_3$–ZnO–Nb_2O_5–Al_2O_3 glasses, J. Non-Cryst. Solids 358 (2012) 11.
[32] S. Li, P. Chen, Y. Li, Structural and physical properties in the system ZnO–B_2O_3–P_2O_5–R_nO_m, Physica B 405 (2010) 6.
[33] N.J. Kreidl, W.A. Weyl, J. Am. Ceram. Soc. 11 (1941).
[34] R.K. Brow, Nature of alumina in phosphate glass: I, properties of sodium aluminophosphate glass, J. Am. Ceram. Soc. 76 (4) (1993) 6.
[35] R.K. Brow, R.J. Kirkpatrick, G.L. Turner, Nature of alumina in phosphate glass: II, structure of sodium aluminophosphate glass, J. Am. Ceram. Soc. 76 (4) (1993) 10.
[36] J. Schneider, S.L. Oliveira, L.A.O. Nunes, F. Bonk, H. Panepucci, Short-range structure and cation bonding in calcium–aluminum metaphosphate glasses, Inorg. Chem. 44 (2005) 8.
[37] J. Tsuchida, J. Schneider, M.T. Rinke, H. Eckert, Structure of ternary aluminum metaphosphate glasses, J. Phys. Chem. 115 (2011) 15.
[38] C. Fu, H.W. Yang, J.J. Wa, C.H. Lai, Y.-M. Lee, C.S. Hsu, P.C. Yang, Structure and property of ZnO content with Tb^{3+} doped zinc aluminum phosphate glass, Appl. Mech. Mater. 117–119 (2012) 4.
[39] D. Massiot, F. Fayon, M. Capron, I. King, S. Le Calve, B. Alonso, J.O. Durand, B. Bujoli, Z. Gan, G. Hoatson, Modeling one- and two-dimensional solid-state NMR spectra, Magn. Reson. Chem. 40 (2002) 7.
[40] D.R. Neuville, L. Cormier, D. Massiot, Al environment in tectosilicate and peraluminous glasses: a NMR, Raman and XANES investigation, Geochim. Cosmochim. Acta 68 (2004) 9.
[41] L. Zhang, H. Eckert, Short- and medium-range order in sodium aluminophosphate glasses: new insights from high resolution dipolar solid-state NMR spectroscopy, J. Phys. Chem. B 110 (2006) 13.
[42] R.K. Brow, C.A. Click, T.M. Alam, Modifier coordination and phosphate glass networks, J. Non-Cryst. Solids 274 (2000) 9–16.
[43] J.L. Rygel, C.G. Pantano, Synthesis and properties of cerium aluminosilicophosphate glasses, J. Non-Cryst. Solids 355 (2009) 8.
[44] B.C. Sales, L.A. Boatner, J.O. Ramey, Chromatographic studies of the structure of amorphous phosphates: a review, J. Non-Cryst. Solids 263&264 (2000) 12.
[45] P. Mosner, K. Vosejpkova, L. Koudelka, L. Montagne, R. Bertrand, Structure and properties of glasses in ZnO–P_2O_5–TeO_2 system, J. Non-Cryst. Solids 357 (14) (2010) 5.
[46] B. Tischendorf, T.M. Alam, R.T. Cygan, J.U. Otaigbe, The structure and properties of binary zinc phosphate glasses studied by molecular dynamics simulations, J. Non-Cryst. Solids 316 (2003) 12.
[47] T. Kubo, J. Cha, H. Takebe, M. Kuwabara, Thermal properties and structure of zinc phosphate glasses, Phys. Chem. Glasses Eur. J. Glass Sci. Technol. B 50 (1) (2009) 4.
[48] J. Schneider, S.L. Oliveira, L.A.O. Nunes, H. Panepucci, Local structure of sodium aluminum metaphosphate glasses, J. Am. Ceram. Soc. 86 (2) (2003) 8.
[49] E. Metwalli, R.K. Brow, Cation effects on anion distributions in aluminophosphate glasses, J. Am. Ceram. Soc. 84 (2001) 1025–1032.
[50] J.M. Egan, R.M. Wenslow, K.T. Mueller, Mapping aluminum/phosphorus connectivities in aluminophosphate glasses, J. Non-Cryst. Solids 261 (2000) 115–126.
[51] N. Troy, Materials and techniques for the femtosecond laser fabrication of optical devices in glass, (Vol. PhD) Applied Science, University of California, Davis, Davis, 2012, p. 67.
[52] L.B. Fletcher, J.J. Witcher, N. Troy, S.T. Reis, R.K. Brow, D.M. Krol, Direct femtosecond laser waveguide writing inside zinc phosphate glass, Opt. Express 19 (2011) 7929–7936.
[53] I. Fanderlik, Optical Properties of Glass, vol. 5, Elsevier, New York, 1983.
[54] J.A. Duffy, M.D. Ingram, An interpretation of glass chemistry in terms of the optical basicity concept, J. Non-Cryst. Solids 21 (1976) 38.
[55] B.N. Nelson, G.J. Exarhos, Vibrational spectroscopy of cation–site interactions in phosphate glasses, J. Chem. Phys. 71 (7) (1979) 9.
[56] L. Popovic, D. de Waal, J.C.A. Boeyens, Correlation between Raman wavenumbers and P – O bond lengths in crystalline inorganic phosphates, J. Raman Spectrosc. 36 (2005) 10.
[57] U. Hoppe, A structural model for phosphate glasses, J. Non-Cryst. Solids 195 (1996) 10.
[58] G. Walter, U. Hoppe, T. Baade, R. Kranold, D. Stachel, Intermediate range order in MeO–P_2O_5 glasses, J. Non-Cryst. Solids 217 (1997) 299–307.
[59] E. Metwalli, R.K. Brow, Modifier effects on the properties and structures of aluminophosphate glasses, J. Non-Cryst. Solids 289 (2001) 10.
[60] H. Ticha, J. Schwarz, L. Tichy, R. Mertens, "Physical Properties of PbO-ZnO-P_2O_5 Glasses II. Refractive Index and Optical Properties", J. Optoelectron. Adv. M. 6 (3) (2004) 7.
[61] P. Chen, S. Li, W. Qiao, Y. Li, "Sturcture and Crystallization of ZnO-B_2O_3-P_2O_5 Glasses", Glass Physics and Chemistry 37 (1) (2011) 29–33.